KU LEUVEN

STADIUS
Center for Dynamical Systems, Signal Processing and Data Analytics

Citation/Reference	Matic V., Perumpillichira Cherian J., Jansen K., Koolen N., Naulaers G., Swarte R.M., Govaert P., Van Huffel S., De Vos M., ``Improving reliability of monitoring background EEG dynamics in asphyxiated infants'', *IEEE Transactions on Biomedical Engineering*, vol. 63, no. 5, 2016, pp. 973-983
Archived version	Final publisher's version / pdf
Published version	http://dx.doi.org/10.1109/TBME.2015.2477946
Journal homepage	http://ieeexplore.ieee.org/xpl/RecentIssue.jsp?punumber=10
IR	https://lirias.kuleuven.be/handle/123456789/509217

(article begins on next page)

Improving Reliability of Monitoring Background EEG Dynamics in Asphyxiated Infants

Vladimir Matić*, Perumpillichira J. Cherian, Katrien Jansen, Ninah Koolen, Gunnar Naulaers, Renate M. Swarte, Paul Govaert, Sabine Van Huffel, and Maarten De Vos

***Abstract*—The goal of this study is to develop an automated algorithm to quantify background electroencephalography (EEG) dynamics in term neonates with hypoxic ischemic encephalopathy. The recorded EEG signal is adaptively segmented and the segments with low amplitudes are detected. Next, depending on the spatial distribution of the low-amplitude segments, the first part of the algorithm detects (dynamic) interburst intervals (dIBIs) and performs well on the relatively artifact-free EEG periods and well-defined burst-suppression EEG periods. However, on testing the algorithm on EEG recordings of more than 48 h per neonate, a significant number of misclassified and dubious detections were encountered. Therefore, as the next step, we applied machine learning classifiers to differentiate between definite dIBI detections and misclassified ones. The developed algorithm achieved a true positive detection rate of 98%, 97%, 88%, and 95% for four duration-related dIBI groups that we subsequently defined. We benchmarked our algorithm with an expert diagnostic interpretation of EEG periods (1 h long) and demonstrated its effectiveness in clinical practice. We show that the detection algorithm effectively discriminates challenging cases encountered within mild and moderate background abnormalities. The dIBI detection algorithm improves identification of neonates with good clinical outcome as compared to the classification based on the classical burst-suppression interburst interval.**

***Index Terms*—Background electroencephalography (EEG), interburst interval detection, neonatal asphyxia, support vector machine (SVM), wavelets.**

Manuscript received May 5, 2015; revised August 7, 2015; accepted August 31, 2015. Date of publication September 14, 2015; date of current version May 19, 2016. This work was supported by the Research Council KUL: CoE PFV/10/002 (OPTEC); IWT: projects: TBM 110697-NeoGuard. The work of V. Matic was supported in part by the IWT Postdoc grant. iMinds Medical Information Technologies SBO 2015, the Belgian Federal Science Policy Office: IUAP P7/19/ (DYSCO, 'Dynamical systems, control and optimization', 2012–2017), and the European Research Council: ERC Advanced Grant: BIOTENSORS (n° 339804). *Asterisk indicates corresponding author*.

*V. Matić is with the Department of Electrical Engineering, KU Leuven, Leuven 3000, Belgium, and also with iMinds Medical IT Department, Leuven 3000, Belgium (e-mail: Vladimir.Matic@esat.kuleuven.be).

P. J. Cherian is with the Section of Clinical Neurophysiology, Department of Neurology, Erasmus MC.

K. Jansen is with the Department of Pediatrics, University Hospital Gasthuisberg.

N. Koolen and S. Van Huffel are with the Department of Electrical Engineering, KU Leuven, and also with iMinds Medical IT Department.

G. Naulaers is with the Neonatal Intensive Care Unit, University Hospital Gasthuisberg.

R. M. Swarte and P. Govaert are with the Department of Neonatology, Sophia Children's Hospital, Erasmus MC.

M. De Vos is with the Institute of Biomedical Engineering, Department of Engineering, University of Oxford.

This paper contains supplemental material available online at http://ieeexplore.ieee.org (File size: 1 MB).

Color versions of one or more of the figures in this paper are available online at http://ieeexplore.ieee.org.

Digital Object Identifier 10.1109/TBME.2015.2477946

I. Introduction

PERINATAL hypoxic ischemic encephalopathy (HIE) is a major cause of morbidity and mortality in newborns [1]. Common neurodevelopmental sequelae in survivors include cerebral palsy, epilepsy, and sensory and cognitive problems [2], [3]. In clinical care of asphyxiated neonates, it is necessary to accurately assess the degree of HIE severity. It is known that clinical neurological examination and cerebral ultrasound perform poorly in this regard. Electroencephalography (EEG) is a widely available noninvasive bed-side test that is exquisitely sensitive for studying abnormalities of the brain function and its recovery in neonatal HIE [4]–[6]. However, the use of continuous EEG (cEEG) monitoring in the Neonatal Intensive Care Units has been limited due to lack of around-the-clock support to interpret this complex signal. Hence, there is an urgent need for the development of real-time systems to automatically quantify neonatal background EEG activity.

The assessment of EEG signals and their dynamic changes enables accurate prognostication in two extreme categories of neonatal HIE. More specifically, the mildest forms of HIE, characterized by normal or mildly disturbed EEG background with preserved sleep-wake cycles are associated with a good clinical outcome. In contrast, severe HIE, characterized by persistent nonresponsive burst-suppression pattern (e.g., Interburst intervals, IBIs$>$10–20 s) and the absence of sleep-wake cycles (at 48 h postpartum) is associated with a poor clinical outcome [7]–[9]. However, compared to these two extreme groups, clinical and EEG assessment of mild and moderate neonatal HIE is challenging.

In clinical practice, to visually score the severity of abnormality of the EEG background in encephalopathic neonates, EEG discontinuity is the most commonly used parameter [7], [9]. This pattern is recognized as higher voltage "bursts" of cerebral activity interrupted by lower voltage "interbursts" [10]. The IBI in neonatal EEG is defined broadly as a pattern with peak-to-peak amplitude $<$25–50 μV. Within this definition, three IBI patterns are identified in full-term neonates: 1) tracé alternant (TA-IBI$>$25 μV)—an EEG pattern present within the quiet sleep stage in healthy newborns; 2) tracé discontinue (TD-IBI$<$25 μV)—a pattern in neonates with mild and moderate HIE; and 3) burst-suppression (BS-IBI$<$5–10 μV)—a pattern in neonates with severe HIE [10]. In the literature, the IBI pattern is usually associated with the classical BS-IBI, defined as a pattern without variability within the suppressed interval. Therefore, a simple amplitude definition threshold is commonly applied: interburst amplitude $<$5–10 μV [7, 11]. On the other hand, mild and moderate EEG discontinuities (e.g., tracé discontinue:

0018-9294 © 2015 IEEE. Personal use is permitted, but republication/redistribution requires IEEE permission.
See http://www.ieee.org/publications_standards/publications/rights/index.html for more information.

TD-IBI) cannot be characterized with such a restrictive definition due to much higher IBI amplitude variability [7] and, thus, their automated detection is more challenging.

Recently, several studies have proposed automated methods to assess the grade of background EEG abnormality in 1-h-long epochs in neonates with HIE. In [12], a combination of quantified EEG (qEEG) features such as EEG discontinuity, amplitude, and frequency content were found useful to assess the severity of HIE in full-term neonates. However, this approach was not successful in differentiating mild from moderate EEG background abnormalities. In addition, other studies have presented algorithms for the detection of BS-IBIs in full term (with severe HIE and IBIs$>$10 s) and premature neonates (EEG consists of simplified burst-suppression patterns) [13]–[17]. These methods use a nonlinear transformation of the EEG signal, followed by a thresholding operator. For instance, the nonlinear energy operator (NLEO), line length, and envelope of the signal are computed on the raw EEG, which are subsequently thresholded. The values above the threshold correspond to bursts, whereas lower values determine the suppressed periods.

However, the quantification of mild and moderate background EEG abnormalities faces three major problems that are not addressed with the previously described automated approaches. First, complex EEG background patterns are often encountered, which consist of varying degrees of EEG amplitude attenuation. Usually, discontinuous EEG periods are intermixed and alternate with continuous EEG periods. As a result, such EEGs cannot be categorized into a simple dichotomy of either burst or suppression patterns as done in neonates with severe HIE or premature neonates. Second, neonatal HIE is not static and EEG background activity evolves over time. At present, there is no automated method which has been developed to quantify the evolution (improvement/deterioration) of the EEG background over longer periods of time (24–48 h). For instance, recovery of severely abnormal EEG background is characterized by a progressive shortening of BS-IBIs and increase in the amplitude of the suppressed periods and change in burst amplitudes [5], i.e., in newborns recovering from HIE, EEGs gradually become more continuous, whereas IBIs evolve from burst-suppression patterns to tracé discontinue and further to tracé alternant patterns. Due to the evolution of encephalopathy, an automated method designed to detect only severe EEG discontinuity (e.g., IBI$>$10–20 s) will no longer function accurately. Third, it is known that the EEG signal is very vulnerable to a various artifacts. Hence, it is important to differentiate whether the output of the thresholding algorithm is an accurate quantification of real burst-suppression-burst complexes or a false detection due to artifacts.

This paper will focus on the detection of definite EEG discontinuities, viz., classical burst-suppression as well as a range of tracé discontinues patterns that express higher interburst amplitudes. We will show that the traditional definition of EEG discontinuity is suboptimal as there is an intrinsic dependence on the duration and the amplitude of the suppressed EEG patterns. This insight will allow us to monitor the evolution of the brain injury and to better model EEG discontinuity, thereby analyzing IBIs with respect to their duration. For this purpose, we will call the patterns analyzed in this study "dynamic interburst intervals (dIBIs)," thereby taking into consideration both the amplitude and the duration of the EEG discontinuity that can evolve over the course of EEG monitoring. Moreover, by detecting definite dIBIs and discarding dubious detections, we develop a system that can be regarded as trustworthy and consistent with a diagnostic interpretation by EEG experts. In addition, we show that using the new algorithm to detect dIBIs, we significantly improve the characterization of neonates with milder encephalopathy and good outcome as compared to a traditionally used classical BS-IBI parameter.

II. Methods

A. Patients

The 53 neonates included in this study were part of a larger cohort of 119 full-term newborns who underwent continuous polygraphic video EEG monitoring (cEEG) as part of a prospective study that evaluated the utility of cEEG monitoring in term neonates with perinatal asphyxia (from March 2003 till August 2007). All EEG data were recorded at the Sophia Children's Hospital, Erasmus University Medical Center, Rotterdam, The Netherlands. The study had the approval of the Erasmus MC Medical Ethical Review Board. Informed consent was obtained from the parents/guardians prior to the start of the registration. The inclusion criteria for EEG monitoring were clinical features of encephalopathy and having at least one of the following features of birth asphyxia: 1) arterial pH of umbilical cord blood $\leq$7.1, and 2) Apgar score $\leq$5 at 5 min. Babies with congenital cardiac abnormalities and multiple congenital anomalies were excluded [18] as well as infants with constantly isoelectric background EEG. This dataset has been used in our recent publications [19]–[21]. The EEG sampling frequency was 256 Hz. The recordings were started 2–48 (median 19) h postpartum, using a set of 17 EEG electrodes, whereas in some patients, a reduced set of 13 electrodes was used. All EEG signals were filtered using high-pass and low-pass FIR filters at 0.7 and 20 Hz, respectively.

B. Datasets

The full dataset was split into three nonoverlapping groups. Dataset **DA** consists of 157 h of cEEG segments from seven neonates with mild and moderate background EEG abnormalities. This dataset was used to optimize the algorithm's parameters for the detection of suppressed intervals (dIBI candidates).

Dataset **DB** consists of cEEG data from 38 neonates. It was used to improve modeling of milder EEG discontinuities and to optimize the refinement postprocessing step. cEEGs of 1-h duration were selected exactly one hour after the beginning of the recording. We did not exclude EEG segments due to the presence of artifacts or epileptic seizures ($n = 18$). The expressed EEG background patterns in this group included mild, moderate, and severe abnormalities.

Dataset **DC** consists of eight neonates with predominantly mild and moderate EEG background abnormalities and was used for the validation of the overall system. We used this

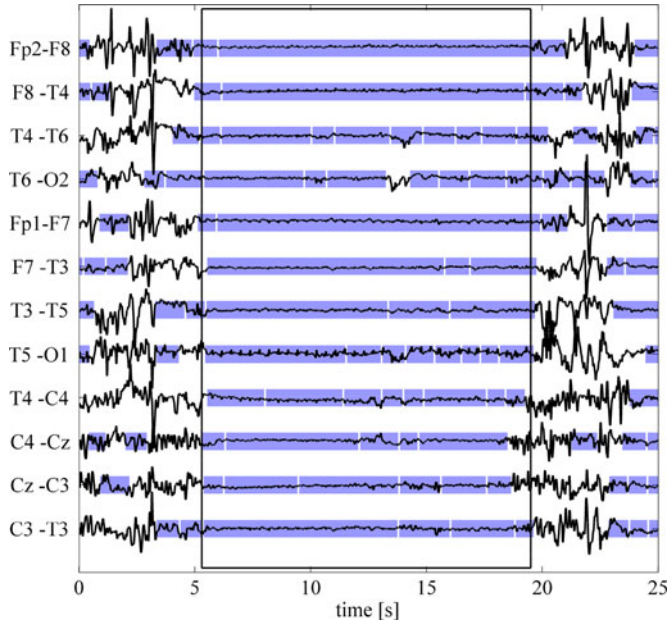

Fig. 1. Classical burst suppression pattern detected in the early stage of the EEG recording. Segments are colored in blue, if the peak-to-peak amplitude of the segment is less than 20 μV.

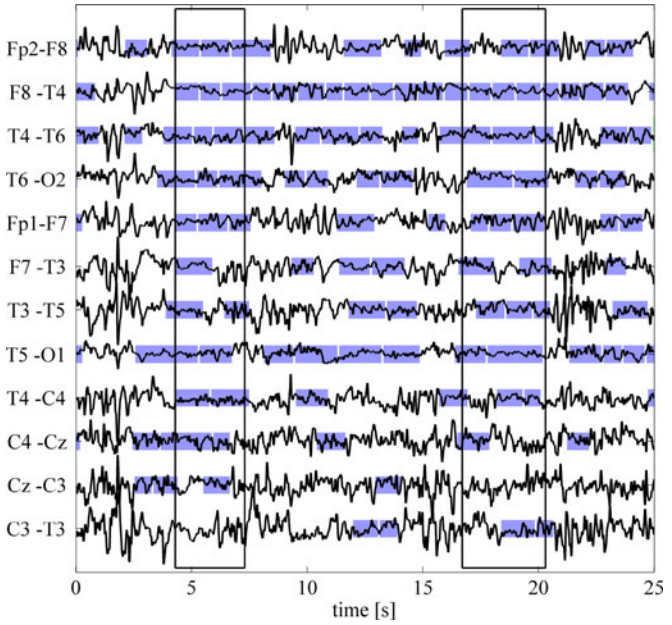

Fig. 2. Detected tracé discontinue patterns with higher interburst amplitudes that evolved over 24 h from patterns shown in Fig. 1.

selection of data for the validation because it is most challenging to accurately detect mild and moderate EEG discontinuities (3 s<dIBI<10–15 s). From each neonate, 30 min of EEG was randomly selected for the analysis.

The visual background grading was performed by an experienced clinical neurophysiologist (PJC), blinded to the clinical details of the neonates. A three-level EEG grading was adapted from Murray *et al.* [9] as follows: 1) normal/mild (IBIs<5 s; poorly organized sleep-wake cycle; recovered, continuous background EEG), 2) moderate (5 s≤ IBIs< 10 s), and 3) severe (10 s ≤ IBIs< 60 s; dominated by prolonged and marked suppressions).

C. Exploratory Definition Of dIBI

In this study, our goal is to develop a system for long-term EEG monitoring of neonatal HIE. Typically, background activity in HIE is characterized by both classical BS-IBI patterns (see Fig. 1) as well as TD-IBIs (<25 μV; Fig. 2). Hence, an ideal quantification would detect both related patterns into a single parameter. The first pattern, burst-suppression-burst complex, is commonly encountered during the initial phase of asphyxia (severe background EEG abnormalities). The second one commonly emerges from classical IBIs after 12–48 h of monitoring in patients showing recovery (mild and moderate background EEG abnormalities). To encompass both severe and mild EEG discontinuous patterns into a unified parameter, we introduce the term dIBI. The word dynamic suggests that EEG discontinuity is characterized with a single parameter despite the fact that interburst amplitude (and overall dIBI morphology) significantly evolves during the recovery/deterioration of hypoxic injuries. The remaining discontinuous EEG patterns, with interburst amplitude >25–50 μV (e.g., tracé alternant) as well as continuous and ambiguous EEG patterns with amplitudes <25 μV are not included into dIBI definition.

Here, we use measures of not only duration (as traditionally done), but also a measure of the dIBI amplitude to characterize EEG background. Therefore, the assessment of the amplitude, not affected by artifacts, needs to be calculated within definite dIBI detections, thereby providing a trustworthy measure.

Our automated approach is developed to first detect attenuated periods of burst-suppression-burst complexes (which we refer to as dIBI candidates). Subsequently, we quantify several features for each dIBI candidate that allow us to distinguish between definite dIBIs and those expressing artifacts/seizures (misclassified—see Figs. 4 and 5). This postprocessing of dIBI candidates is crucial for reliable background quantification. In addition, it may happen that EEG is both highly variable and attenuated, and that visual interpretation of IBI duration is quite challenging. In such cases (see Fig. 3), we say that the EEG is ambiguous. Without the refinement step, falsely prolonged detections may appear and jeopardize the automated diagnostic grading of the severity of encephalopathy (see Figs. 3 and 6). This is commonly encountered in cases when the EEG is evolving from tracé discontinue patterns to normal (continuous) background EEG and an automated system can falsely classify a recovering neonate as being very sick. In order to decide whether a dIBI candidate should be included into further statistics or not, we will train machine-learning classifiers for this task.

D. Detection of dIBI Candidates

To detect suppressed periods, EEG channels are independently adaptively segmented with an algorithm proposed in [22]. The main goal of the segmentation step is to distinguish and

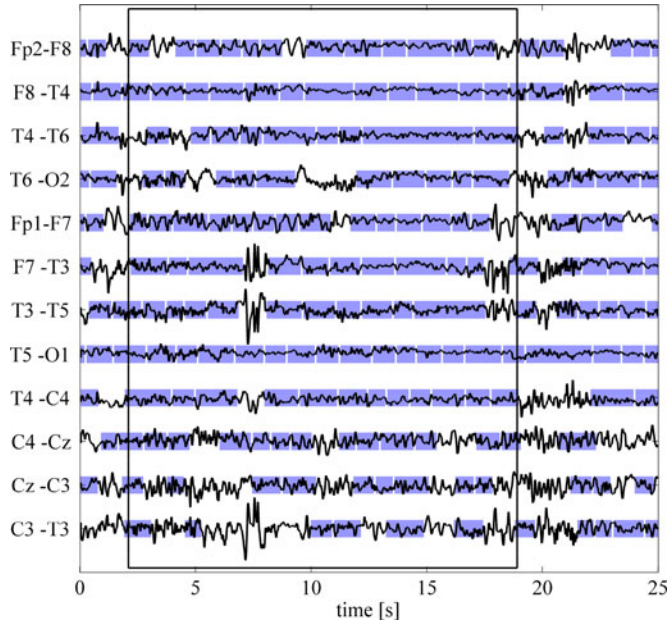

Fig. 3. Ambiguous EEG pattern occurring close proximity in time to the patterns in Fig. 2. These types of detection were excluded as they do not express clearly distinguishable burst-suppression-burst complexes.

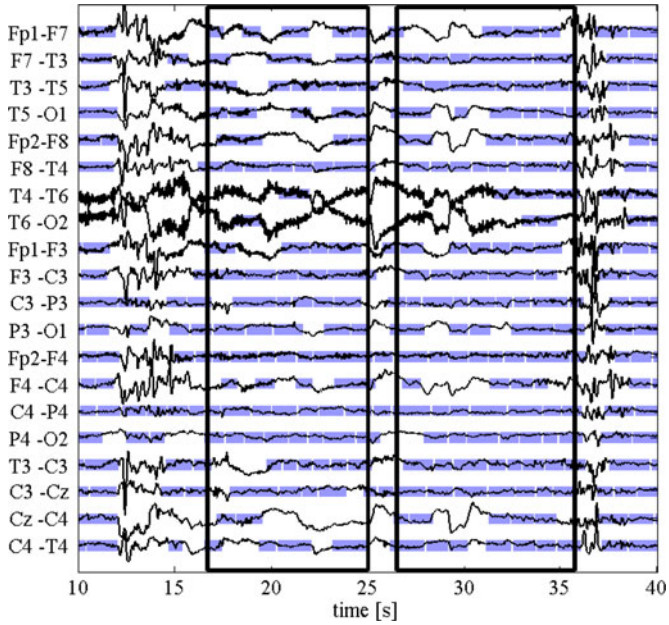

Fig. 5. Artifact interrupts the suppressed interval, thereby falsely shortening dIBI duration and amplitude assessment. Instead of a single longer dIBI, two shorter dIBI candidates are falsely detected.

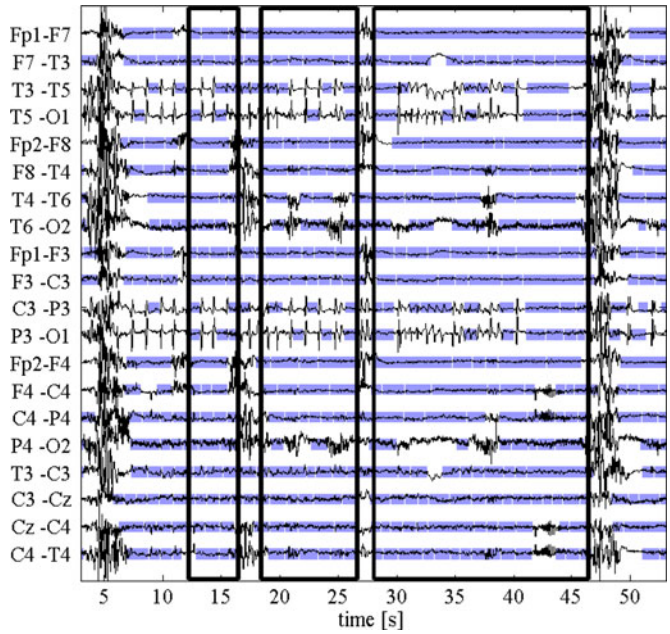

Fig. 4. Examples of false-positive dIBI detections that are produced by epileptic seizure activity over T5 and P3 electrodes.

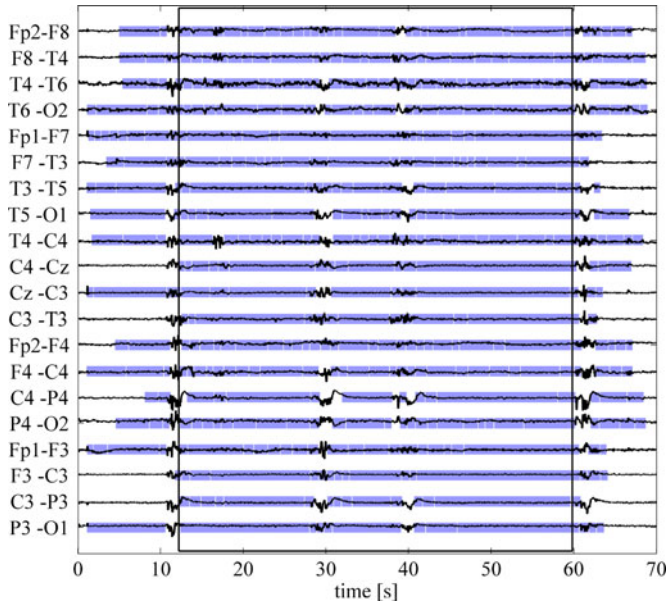

Fig. 6. Bursts with very low amplitudes ("peak to peak" $< 20\ \mu$V) are missed by the detection algorithm, producing falsely prolonged dIBI detection.

separate locally suppressed EEG periods from burst periods [see Fig. 7(A1)]; [23]. Subsequently, we classify segments into the low-amplitude class (L) if the segments' "peak-to-peak" amplitude is below 20μV [see Fig. 7(A2)]; for more details, see [23].

To detect globally suppressed EEG periods after the segmentation/classification step, we monitor the spatial and temporal distribution of low-amplitude segments across EEG channels. To accomplish this, we count the number of EEG channels expressing low-amplitude segments at a particular time instant [see Fig. 7(A3)]. This results in a new signal, which we call low-amplitude temporal profile (LTP). Consequently, we define a dIBI candidate if the LTP signal exceeds half of the total number of EEG channels for more than 3 s. This results in a large number of static detections, which can be either definite dIBIs or misclassified dIBIs that fulfill the thresholding

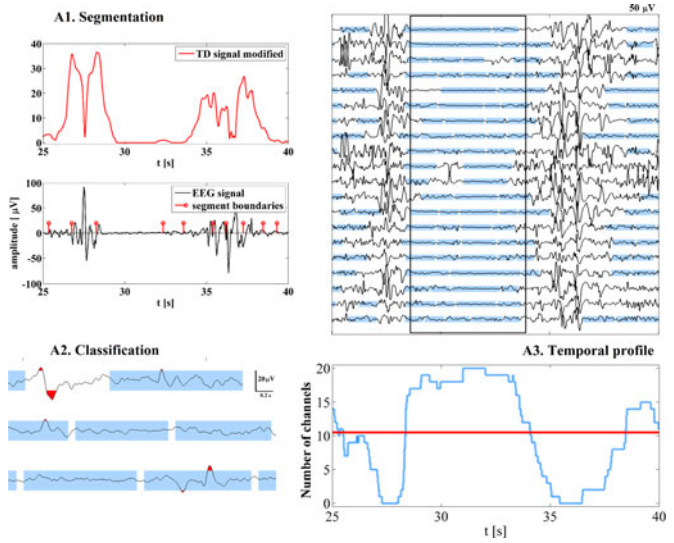

Fig. 7. Three main steps for the detection of the suppressed EEG intervals (dIBI candidates) are illustrated. (A1) Adaptive segmentation of the EEG is done. Maximum values of the "TD" signal define EEG segment boundaries (see [23]). (A2) Classification of short segments into low amplitude class is done. (A3) Spatial distribution of the low-amplitude segments is calculated. This signal, LTP is thresholded (red horizontal line) and dIBI candidates are detected (marked with black rectangle).

requirements. Examples of definite detections are given in Figs. 1 and 2, whereas misclassified dIBIs are shown in Figs. 3–6.

E. Reliable Detection of Definite dIBIs

The algorithm uses machine-learning techniques to distinguish definite and misclassified dIBI detections. For every detected dIBI candidate, a set of parameters is calculated that quantifies dIBI detection certainty. Thirteen parameters are implemented as a heuristic translation of visual analysis done by an experienced PJC while assessing whether dIBI candidates are definite or dubious (misclassified) dIBIs. These parameters quantify in a mathematical way the level of dIBI amplitude, the number of EEG channels that show suppression, the largest duration of suppression along a single channel, and the presence (existence) of borderline bursts for a detected suppressed period. In Fig. 8 for two dIBI detections (upper traces), we illustrate how one of the features, the presence of borderline bursts, is examined. For this purpose, we used the discrete wavelet transform (DWT), which is suitable for the detection of a transitioning point (see Fig. 8 lower traces). Wavelet coefficients at the decomposition level 2–5 (4–32 Hz mainly) are expected to have higher absolute values for burst periods as compared to suppressed periods (flat EEG or very smooth oscillations). Next, we compare 3 s of the burst part versus the 3 s of the suppressed interval. The majority of large absolute wavelet coefficients values if contained within the burst part would imply the accurate detection of a transitioning point. For instance, this will be the case for the definite dIBIs in Figs. 1 and 2, but less likely for the dubiously detected transitions in Figs. 3–6. For the full mathematical definitions of all 13 parameters, see the Appendix.

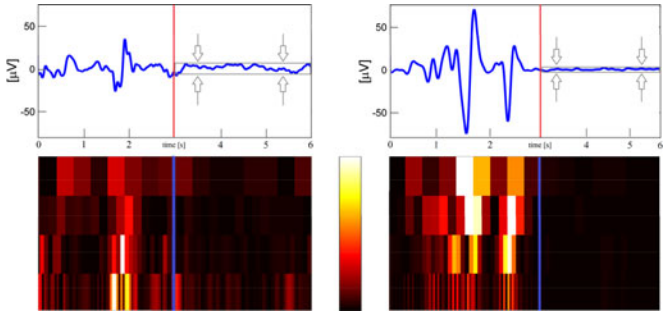

Fig. 8. Two transitioning points (vertical lines, above [red] and below [blue]) are illustrated for milder EEG discontinuity (dIBI$<$10 s; left) and for severe EEG discontinuity (dIBI$>$10 s; right). Note that for the shorter dIBI amplitude of the suppressed part shows more variability and the transitioning point is more challenging to be validated. On the other hand, longer dIBI (classical burst-suppression) shows nonresponsive amplitude, thereby making recognition of definite dIBIs much easier.

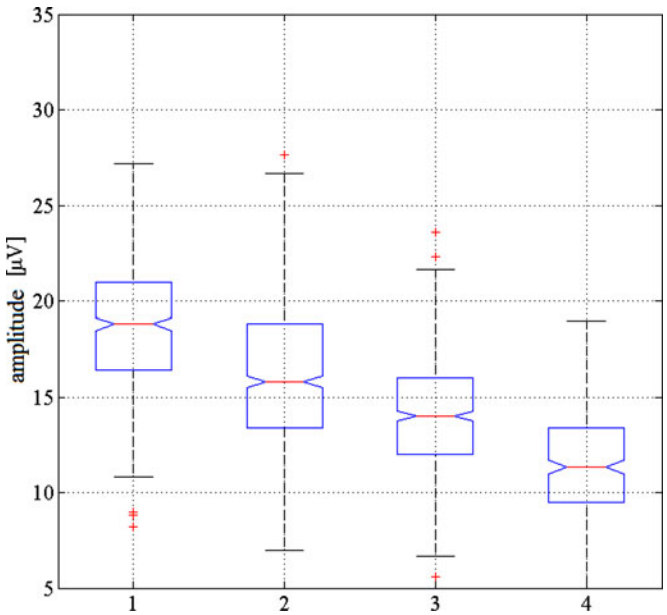

Fig. 9. Amplitude distribution of definite dIBIs is depicted for each dIBI duration group. Group I: 3 s$\leq$dIBI$<$5 s; Group II: 5 s$\leq$dIBI$<$10 s; Group III: 10 s$\leq$dIBI$<$20 s; Group IV: 20$\leq$dIBI ($<$40 s). A one-way ANOVA test with Bonferroni correction showed a significant difference in the mean amplitude distribution (F-statistic $=$ 337.8, $p<0.001$).

Furthermore, due to encountered differences in dIBI morphology with respect to its duration, we suggest categorizing all definite dIBIs into four duration-related groups as follows (1):

$$\mathrm{dIBI} = \begin{cases} \text{group I}, & 3\mathrm{s} \leq \mathrm{dIBI} < 5\mathrm{s} \\ \text{group II}, & 5\mathrm{s} \leq \mathrm{dIBI} < 10\mathrm{s} \\ \text{group III}, & 10\mathrm{s} \leq \mathrm{dIBI} < 20\mathrm{s} \\ \text{group IV}, & 20\mathrm{s} \leq \mathrm{dIBI}(< 60) \end{cases}. \quad (1)$$

We can see that shorter definite dIBIs have higher amplitude, whereas longer ones show more suppressed amplitude (see Fig. 9). This amplitude-duration interdependence enables enhanced modeling of EEG discontinuity.

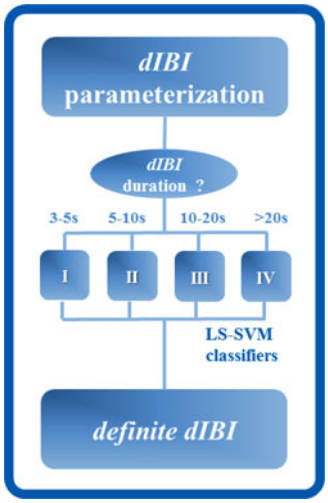

Fig. 10. Flowchart of the algorithm for automated detection of definite dIBIs. The detected dIBI candidate is parameterized and obtained values are used as classifiers' input feature vectors. To optimally account for diverse duration-related dIBI morphological differences, four different LS-SVM classifiers are independently optimized. They make a decision whether a dIBI candidate is definite dIBI and whether it should be used for EEG quantification. Uncertain detections are excluded from further EEG analysis as misclassified dIBIs.

Next, the parameters that quantify dIBI candidates are used as input feature vectors into least-squares support vector machine (LS-SVM) classifiers [24]. Initially, we optimized only one LS-SVM classifier. However, shorter dIBIs with higher interburst amplitudes were more challenging for the classification than longer dIBIs (data not shown). Therefore, four LS-SVM classifiers are used to enhance the classification accuracy and to adjust the algorithm to the dynamic changes/evolution of the EEG discontinuity (TD-IBIs are shorter with higher amplitude compared to BS-IBIs). The state flow of the complete algorithm is illustrated in Fig. 10.

The objective of the classifiers is to estimate whether a newly detected dIBI is definite—{1} or misclassified—{0}. To optimize classifiers, four mutually exclusive training datasets were created depending on dIBI duration by randomly selecting 80% of dIBIs. The remaining 20% of dIBIs from each group were used to test the corresponding LS-SVM classifiers. The LS-SVMlab v1.8 toolbox implementation was used in this study (www.esat.kuleuven.be/sista/lssvmlab, [25]). In all cases, a Gaussian kernel was applied. Tuning of the parameters was conducted in two steps. First, coupled simulated annealing was performed [26] and afterward, a second optimization procedure (simplex) was applied to perform a fine-tuning step. The fivefold cross-validation misclassification error was used as an optimization criterion.

III. Results

A. Dataset DA

The initial detection algorithm, including adaptive segmentation, amplitude-based classification, and dIBI detection, was optimized using a training dataset DA. In total, 157 h of cEEG from seven neonates was processed and analyzed. The 18802 detected dIBIs were visually checked for precise burst/suppression transitioning in each channel and for accurate detection of dIBI duration. This meticulous evaluation of EEG discontinuity patterns enabled us to optimally set and fix the parameters of the algorithm for the detection of dIBI candidates. We do not present statistics for this dataset as it was used for the tuning of the processing algorithm. Nevertheless, although we improved our initial version of the algorithm ([23]; average rate of misclassified dIBIs was 30–50%), the false positive detection rate remained unacceptably high.

B. Dataset DB

A test dataset DB is processed with the algorithm to further study definite, correctly detected dIBIs. Using the initial algorithm, 4408 dIBI candidates were detected within 38 h of cEEG. After visual checking of these detections, 2273 dIBIs were marked as definite dIBIs, whereas 2135 dIBIs were excluded from further analysis as misclassified (false positive and dubious ones).

Subsequently, LS-SVM classifiers were trained to optimally match the visual classification done by the PJC. The total number of dIBIs per duration group was: 1239 (3 s$\leq$dIBI$<$5 s), 1382 (5 s$\leq$dIBI$<$10 s), 881 (10 s$\leq$dIBI$<$20 s), and 906 (dIBI$\geq$20 s). The performance of the classifiers is illustrated using receiver operating characteristic (ROC) curves (see Figs. S1 A-D in the supplemental data). High area under the ROC curve values (AUC) are achieved for all four classifiers: 0.91, 0.94, 0.94, and 0.97, implying that high discrimination between definite and misclassified dIBIs has been achieved. The highest AUC was achieved for the class with longest dIBIs (BS-IBI), which implies that these dIBIs have a more definite (simpler) morphology.

Next, it is important to show how four classifiers would work in the clinical practice. The working points of the ROC curves are selected using the "rate of misclassification" error criteria (see Figs. B1 A-D). We show the percentage of true positive and false positive detections after the refinement step (see Fig. 11). We can see that large number of definite dIBI detections will be kept after the refinement step, which is essential for further statistical analysis (e.g., median dIBI; histogram). Furthermore, the false positive detection rate has decreased per dIBI duration group from (61%, 44%, 36%, and 55%) to (28%, 17%, 14%, and 16%), respectively.

C. Validation of the Complete Algorithm

To illustrate how powerful the complete algorithm is, the validation results are shown in an independent validation dataset DC. First, an experienced clinical pediatric neurologist visually marked dIBIs, allowing higher dIBI amplitude as compared to BS-IBIs and excluding detections whose duration was difficult to be interpreted. Next, the EEGs were processed with the automated algorithm and the results were compared. Table I illustrates that after detection of dIBI candidates without the postprocessing step, good results have been obtained, but the number of misclassifications was rather high as compared to the EEG expert. After the postprocessing step, and the analysis of

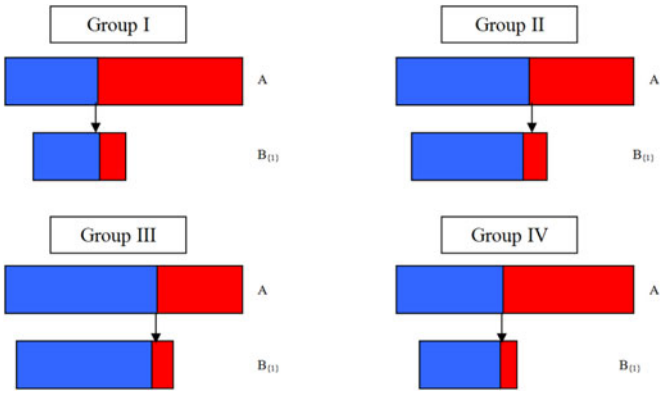

Fig. 11. For each of the four duration-related dIBI groups (as defined in Fig 9) in dataset DB, the first bar (A) represents the distribution (%) of automatically detected definite dIBIs (blue, true positives) and misclassified ones (red, false positives) compared to the visual marking by the PJC. After the refinement step using LS-SVM classifiers, a reliable subset ($B_{\{1\}}$) of dIBIs is generated for each group, resulting in a significant improvement in the percentage of definite dIBIs.

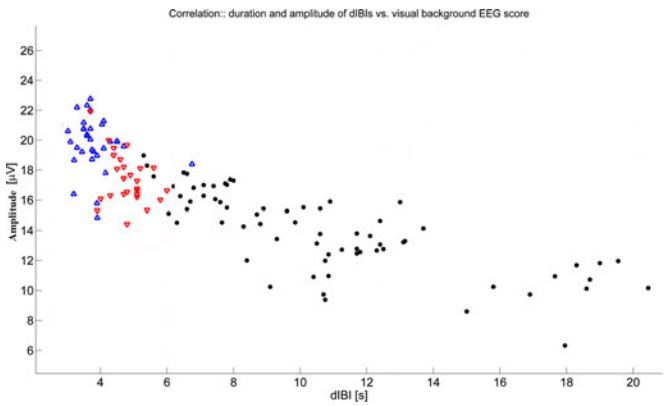

Fig. 12. Output of the complete algorithm is compared with the background EEG abnormalities visually graded by a PJC. Median duration and amplitude of definite dIBIs detected within 1 h of cEEG are plotted as a single data point (four data points per neonate). Background EEG abnormality of the corresponding 1-h epoch is scored by the PJC as mild (blue), moderate (red), or severe (black).

TABLE I
RESULTS OF AUTOMATED DEFINITE DIBI DETECTIONS IN A NEW DATASET DC AS COMPARED TO THE VISUAL SCORING

dIBI group	Detected dIBI candidates	*Definite* dIBIs marked by the rater	True positive rate after the refinement step		False positive rate after the refinement step	
I	280	189	125/128	(98%)	3/91	(3%)
II	330	254	202/209	(97%)	7/76	(9%)
III	169	126	90/102	(88%)	12/43	(28%)
IV	56	32	19/20	(95%)	1/24	(4%)
Total	835	601	436/459	(95%)	23/234	(10%)

First, the algorithm detected dIBI candidates (both definite and misclassified) and this is presented in the second column. The number of visually scored definite dIBIs is presented in the third column. After the refinement step, the algorithm retains definite dIBIs which are compared with the visual scoring. The true-positive rate (%) is presented in the fourth column, whereas the false-positive rate (%) is presented in the fifth column. The results are presented for four dIBI duration groups and the total number of detections is given.

definite dIBIs, high true positive rates are achieved : 98%, 97%, 88%, and 95%, while the false-positive rate remained very low, demonstrating the high reliability of the algorithm.

D. Benchmarking: dIBI Duration and Amplitude Versus Expert Visual Background EEG Scoring

The main objective of our automated system is to apply it as an assistive decision-support system to assess the severity of EEG background discontinuity. Here, we show the results of fully automated processing of cEEG epochs within dataset DB (38 neonates). From each neonate, we equidistantly selected four 1-h cEEG segments across the whole EEG recording (minimum distance between segments longer than 4 h). An experienced PJC visually assessed background EEG of these neonates. The EEG from some neonates cannot be described with only one class due to evolution of the background activity. For instance, the background EEG abnormalities of a neonate with recovering HIE may be graded as: severe (21–22 h postpartum-PP), severe (27–28 h PP), moderate (33–34 h PP), and mild (39–40 h PP).

Furthermore, within each 1-h EEG segment, median duration and median amplitude of dIBIs were automatically calculated to characterize the trend of the EEG background activity. This is shown in Fig. 12, where each data point corresponds to a 1-h cEEG segment (four data points per neonate).

Next, we calculated the Spearman correlation coefficient between background EEG grades and median dIBI duration ($\rho = 0.3718, p < 0.001$) and between background EEG grades and median dIBI amplitude ($\rho = -0.449,\ p < 0.001$). Introducing dIBI amplitude as a feature, we enhanced the separation between the classes compared to the use of only duration of dIBIs. In particular, this can be observed in the separation between mild and moderate classes. Therefore, incorporating a trustworthy measure of dIBI amplitude enabled high agreement with background EEG scores as done by the PJC.

At this stage, during the development phase of the algorithm, we have restricted ourselves to median dIBI duration and amplitude, and do not aim to perform comprehensive automatic grading (classification) of the background EEG activity. For the latter, many other parameters need to be taken into account such as frequency content, morphology and variability of EEG bursts, sleep-wake cycles, EEG symmetry, synchrony, and presence of sharp waves.

IV. DISCUSSION

The goal of this study was to develop an automated method for a reliable assessment of a broad range of background EEG discontinuities in full-term asphyxiated neonates. To the best of our knowledge, this is the first study that used an automated method to study EEGs over long monitoring hours and to accurately detect milder EEG discontinuities. These patterns are predominantly encountered in neonates diagnosed with mild and moderate HIE. This subgroup of HIE neonates still represents a great challenge for clinicians aiming to standardize a visual grading system for their systematic study and to predict their

neurodevelopmental outcome [31]. In this context, we defined a new, visually interpretable parameter, dIBI, as an extension of the classical BS-IBI concept. In general, dIBI can be seen as a burst-suppression-burst pattern with evolving activity encountered during both the suppressed and burst periods. In addition, apart from temporal information, the novelty of dIBI is that it incorporates various interburst amplitude levels.

The postprocessing step, estimates diverse dIBI amplitude values, and accordingly, we optimized four LS-SVM classifiers. In this way, we improved the detection accuracy compared to the use of only one classifier. It is also noteworthy that not only the amplitude, but also the overall dIBI morphology is different depending on duration. For instance, for dIBIs$<$10 s, the transition points of burst/suppression are milder and more gradual. In contrast, burst/suppression alternations for dIBIs$>$20 s are much more pronounced and abrupt. Last but not the least, the postprocessing step enables analysis of a wide range of encountered discontinuous background EEG states in neonates with HIE. Hence, manual data preselection by clinicians is not needed and the algorithm can be used for long-term continuous monitoring. In contrast, some of the published algorithms are developed to process and tackle only markedly discontinuous/burst-suppression EEG states [13], [14], [17]. With our algorithm, milder "discontinuous" tracé alternant pattern and continuous EEG patterns can be processed as well without affecting the algorithm's performance.

Few research groups have attempted to develop methods for automated grading of background EEG abnormalities in full-term asphyxiated neonates. A notable contribution are the literature works [13] and [27], where a method for suppression/burst detection has been developed. As the first step, the method first detects "burst-suppression" states and then quantifies the background EEG with an IBI detector. However, mild to moderate EEG discontinuities were not analyzed in those studies, which is a significant limitation. Moreover, for the development of their method, the researchers included only a small number of neonates (six), expressing only prolonged BS-IBIs ($>$10 s) [27]. In a follow-up validation study of this method [28] in 21 neonates, a highly dichotomous separation of neonates into "good" and "poor" outcome groups has been achieved using detected median IBI values. It is surprising that none of the neonates showed recovery and evolution of background EEG (although nine were clinically judged to have mild-moderate HIE and later had good clinical outcomes). On the other hand, our algorithm is able to ascertain a continuous and gradual transition of background EEG states as we have implemented detection of milder discontinuities as well.

Other automated detection methods have studied "burst/suppression" patterns in premature EEG [14]–[17]. Compared to these, the dIBI parameter includes more complex burst-suppression-burst patterns, thereby encompassing a broader range of EEG discontinuities. In addition, the number of dIBI patterns that we analyzed is at least ten times higher, covering many more hours of EEG recordings. The aforementioned methods can be compared with the first part of our algorithm for detection of dIBI candidates. They are all designed to "threshold" either suppressed or burst EEG periods. However, these studies have not addressed and explored the adverse effects of artifacts/seizures that can interrupt the suppressed periods and be erroneously detected as bursts. In addition, we aimed to identify a large set of correctly detected definite dIBIs that would be confirmed with high interrater agreement. As part of this strategy, uncertain and ambiguous EEG patterns would be excluded, reducing significantly the number of misclassified detections.

Due to recovery of brain injury and background EEG evolution in mild and moderate HIE, dIBIs significantly change in morphology and makes detection rather challenging. At the beginning of the recordings ($<$24 h postpartum), burst periods tend to be low in amplitude (e.g., pure theta activity $<$10–20 μV [6]), with extremely attenuated suppressed segments. When the EEG background improves along with recovery from HIE, the amplitude of both suppressed and active burst periods would increase, whereas the duration of dIBIs would decrease. Hence, the encountered scenarios may include bursts registered at 12-h postpartum that are lower in amplitude than suppression segments at 48-h postpartum. This will result in an overlap between suppression/burst periods at various time points that static burst/suppression detection algorithms will not be able to distinguish. For instance, qEEG parameters (mainly amplitude based) used for supervised learning (e.g., [13]) will be insensitive to detect such changes in EEG morphology. In contrast, dIBI candidates are detected with high sensitivity and the presence of borderline bursts is examined afterward. Here, the algorithm compares how burst/suppression patterns are relatively distinguishable regardless of their amplitude values (see parameter transitioning in the Appendix). Subsequently, as dIBIs become shorter with higher amplitude activity visible during suppressions, a corresponding duration-related LS-SVM classifier would be applied to classify them as definite dIBIs. Approaches presented in [13]–[15] are not sensitive to the evolution of background EEG activity. On the other hand, our method is adaptable to dynamic changes in the background EEG, which is a distinct advantage.

In [12], authors proposed a method to quantify background EEG without direct assessment of EEG discontinuity. The authors showed that a combination of qEEG features can be applied to assess background EEG abnormality as determined by experienced PJCs within 1-h segments of EEG. The method is designed to replicate experts' grading of HIE severity, resulting in a single-output value. Generally, this value represents a grade from 1 to 4 (mild, moderate, severe, or isoelectric), which helps to partly replace visual EEG classification. However, this output, which uses a combination of many qEEG features, does not reveal new insights into the various characteristics of EEG discontinuity in neonatal HIE. In contrast, our automated output offers more insight than just four discrete values. Therefore, the speed of EEG improvement/deterioration can be evaluated more effectively using a dIBI amplitude-duration plot. For instance, a neonate who is recovering from severe HIE could be initially simply be graded as 3 (severe) according to the approach described by Korotchikova [12], whereas in dIBI amplitude-duration plot (see Fig. 12), we will be able to observe progressive dIBI duration shortening and amplitude increase. In other

words, our method enables finer monitoring of the speed of the HIE recovery, which is known to be a very important clinical parameter. Moreover, it is also difficult to estimate how the proposed systems [12] would tackle many hindrances like artifacts and seizures, which were manually excluded in that study. According to the authors, the EEG datasets were preselected and represent ideal-like scenarios with consistent background EEG grades. Compared to this study, our dataset included major artifacts and electrographic seizures, and used nonpreselected EEG segments, representing real-life scenarios.

By introducing the concept of dIBI amplitude measure, we achieved better background EEG quantification compared to the classical BS-IBI. According to our analysis, BS-IBI was mainly suited for quantifying EEGs in neonates expressing severe background abnormalities and poor clinical outcome [18]. On the other hand, neonates recovering from HIE with improving background EEG lacked a suitable quantified parameter for their characterization. Here, we have shown that dIBI can accurately quantify milder background EEG discontinuities. Neonates persistently showing these milder EEG abnormalities had no thalamus-basal ganglia injuries on magnetic resonance imaging (MRI) and, subsequently, had good clinical outcomes [18]. In addition, our findings corroborate the results of previous studies that visually studied amplitude differences in discontinuous EEG patterns in full-term neonates with HIE. Pezzani [6] analyzed EEG recordings within the first 24 h of life and found that neonates with HIE and nonresponsive EEG suppressed intervals (<5 μV) died or developed severe sequelae. In contrast, infants expressing higher interburst amplitudes of 5–10μV survived without any sequelae. In another study [29], researchers analyzed suppressed EEG intervals in term neonates with HIE and their relationship with clinical outcome. In particular, they defined classical BS-IBI with the amplitude consistently <5 μV ($n = 15$ neonates) and "modified BS-IBI" expressing higher interburst amplitude >5 μV ($n = 8$ neonates). The neonates expressing "modified BS-IBI" showed more favorable outcome compared to the BS-IBI group. In another study [7], the authors analyzed discontinuous EEG intervals that could not be classified as classical BS-IBIs. This study included neonates with HIE up to seven days postpartum, and, therefore, their findings cannot be directly compared with ours. However, the expressed trends appear to be similar, and higher interburst amplitudes implied a more favorable clinical outcome.

V. Conclusion

Finally, even though our definition of dIBI incorporates amplitude and duration, and takes into account the various types of transitioning between bursts and dIBIs, it could be argued that an attempt to represent a complex and chaotic signal like EEG with a single parameter is fundamentally flawed. However, in encephalopathic neonates, we would expect a relative simplification of EEG patterns, resulting in discontinuity of the EEG and the appearance of definite dIBIs which would be detected by our automated system. Since our aim with automated dIBI detection is to develop a method to grade HIE, and monitor its evolution in neonatal encephalopathy and not to encapsulate the entire range of complexities of the EEG signal from normal to abnormal, we feel that our approach is justified. Furthermore, the advantage of our refinement step is that it selects only highly certain dIBI detections, which would have very good interrater agreement. To further investigate the potential of the dIBI parameter for scoring background EEG abnormalities and its prognostic value, it is necessary to perform further multicenter validation studies with even larger datasets and characterizing patterns of brain injury on MRI and clinical outcome. This analysis could also lead to a widely acceptable EEG background grading system in HIE using data-driven rules and become an important aid in guiding treatment decisions.

Appendix
Framework for the Reliability Parameterization of dIBI

To distinguish definite dIBI detections according to the detection certainty, we parameterize the "burst-suppression-burst" complex. These parameters are developed to characterize the classification process done by a PJC to confirm definite dIBIs. Some of the parameters are optimized to confirm definite dIBIs, whereas others are adjusted to exclude misclassified dIBI detections. We provide a detailed description of the reliability parameters and illustrate how they are calculated within the burst-suppression-burst complex in Fig. 13.

The following parameters are used to parameterize every detected dIBI candidate.

1) Suppression (one parameter) is defined as a single median value of the rectified EEG signal within the suppressed dIBI period across all EEG channels.
2) Flatness (four parameters) is calculated for each EEG channel independently within the suppressed dIBI period. We adjusted two horizontal border lines, so that they enclose 95% of all EEG samples within the dIBI. The minimum possible distance between these two horizontal lines represents the parameter flatness (see Fig. 14). Next, the flatness is calculated for each EEG channel and the obtained values are sorted into the ascending order. Subsequently, these values are split into four equal groups. For each group, a median value is calculated, resulting into four parameters that estimate the suppression level of the dIBI.
3) Longest (four parameters) within the dIBI, for each EEG channel, we calculate the longest interval of the low-amplitude segment (L) classes that are not interrupted by a higher amplitude activity (see Fig. 13). If several consecutive low-amplitude segments are present next to each other, we will merge them into a single one. This parameter ranges from 0% (no low-amplitude segments) to 100% (only low-amplitude segments). It is an important descriptor for decisions whether the dIBI suppressed period is interrupted, especially in cases when higher amplitude EEG activity is distributed randomly across the suppressed period. Similar to the parameter flatness, we sort all values calculated for each channel in the ascending order and calculated four parameters as median value of the corresponding quartile groups.

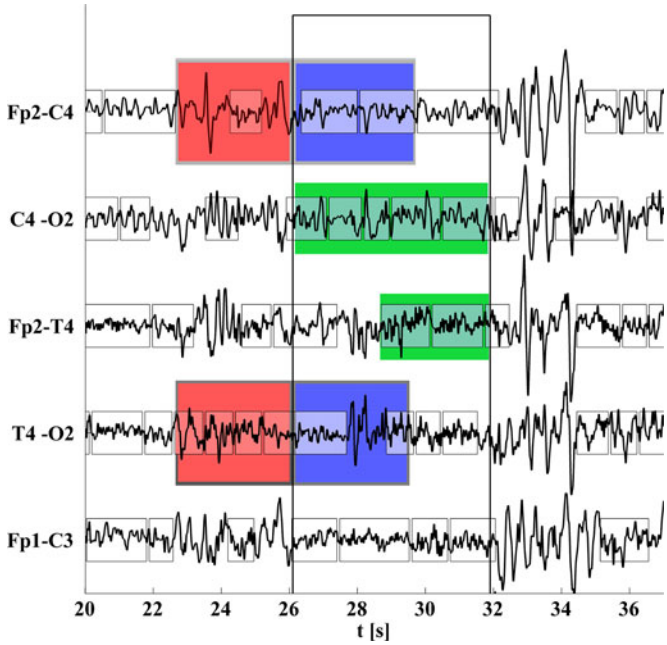

Fig. 13. Detected dIBI candidate is marked with large black rectangle, whereas low-amplitude segments (L) are marked with smaller ones. The reliability parameter transitioning examines the dIBI segmentation accuracy and the certainty of the complete complex burst-suppression-burst. For each channel, 3s of the burst part (red) and 3s of the suppressed part (blue) are compared. Here, only two such examples are illustrated with red/blue rectangles. In addition, an illustration of the parameter longest is depicted in green. It calculates the longest possible duration of the consecutive segments with low amplitude (L) within dIBI. In channel C4-O2, this value is maximal ($=1$), whereas for the channel Fp2-T4 this value is 0.5 (50% of the duration of dIBI candidate). Parameter longest is useful to exclude ambiguous EEG discontinuity and other uncertain detections.

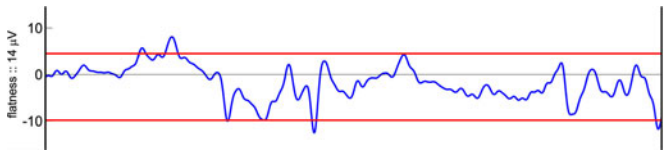

Fig. 14. Illustration of how the parameter flatness is calculated within the suppressed dIBI part (4 s long) for a single channel. Two horizontal red lines are adaptively adjusted until they meet two criteria. First, they need to enclose 95% of the signal samples. Second, the calculated distance between them has to be minimal. In this example, the calculated distance is 14 μV.

4) Number of channels (one parameter): For the presumed duration of the dIBI (suppressed part), we calculate the mean value of the LTP signal. Next, this value (number of EEG channels expressing LTP signal) is divided with the total number of (bipolar montage) EEG channels. As dIBI was thresholded at a value of one more than half the number of total EEG channels, this parameter will be in the range from 55% to 100% (0.55–1).
5) Transitioning (two parameters): This parameter examines the presence of bursts and how distinguishable burst/suppression segments are. Six seconds of the EEG signal are selected with a center exactly at the detected burst/suppression transition point. In Fig. 13, burst parts (red) and suppressed parts (blue) are marked. Next, this signal is decomposed using the DWT [30]. We applied Daubechies four mother wavelet and five levels of decompositions. In this way, the burst part (3s) is characterized with wavelet coefficients that express higher absolute values, whereas the suppressed part (3s) is characterized with wavelet coefficients close to zero (see Fig. 15, middle plot). To further enhance the differences between burst and suppression segments, we sort absolute values of wavelet coefficients into the ascending order. Then, iteratively, starting from the smallest values, we set small wavelet coefficient values to zero. We repeat this process while keeping more than 90% of the original signal power within the remaining wavelet coefficients (see Fig. 15, bottom plot). In this way, the approximated signal (in Fig. 15, upper plot—marked in black) preserves the active burst period, whereas the majority of wavelet coefficients within the suppressed period are set to zero. The percentage of power

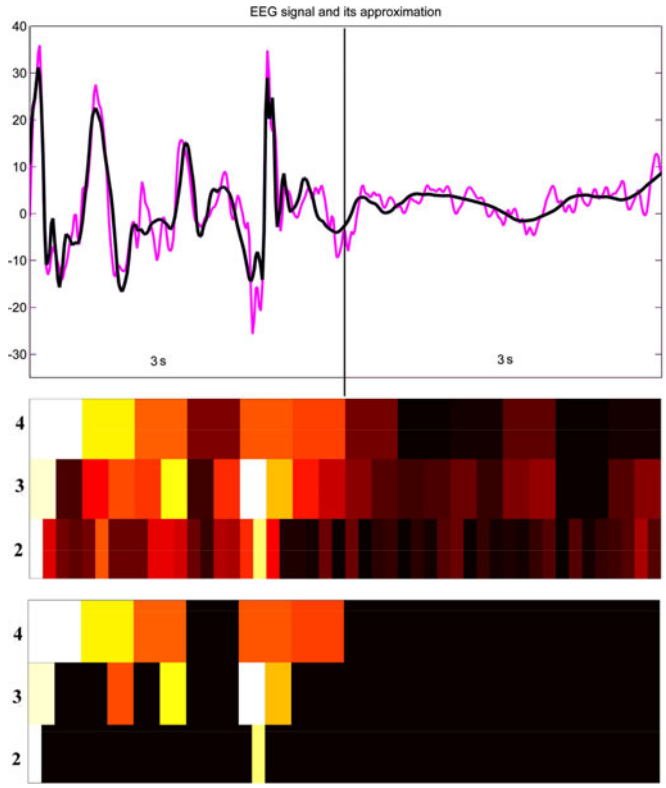

Fig. 15. Transitioning parameter is illustrated for detected EEG discontinuity. The first 3 s of the signal represents a burst period, whereas the last 3 s corresponds to the suppressed segment (upper plot: purple-original EEG signal, black-approximated EEG signal). In two lower figures, wavelet coefficients (levels from 2 to 4 are displayed as they carry the largest portion of the signal power) are depicted in black for zero values, and in white and yellow for larger absolute coefficient values (middle plot). After sparse approximation, large wavelet coefficients would be retained mainly within the dynamic burst period (bottom plot). Therefore, in this example, the parameter *transitioning* (value close to 1) would imply that the vast majority of the high activity is localized within the left (burst) part of the signal, whereas the right part (suppression) does not contain any significant component of EEG activity with higher frequencies. In this way, the high energy coefficients (colored in white) capture the "high activity burst" behavior as compared to the suppressed periods where such activity is lacking. Therefore, the calculation of the transitioning parameter efficiently characterizes the presence of distinguishable burst/suppression alternations.

retained by wavelet coefficients within the burst part compared to the total power of all wavelet coefficients, after the sparse approximation, determines the transitioning parameter. Furthermore, this parameter is averaged across all EEG channels. Thus, if the burst/suppression transition represents a clear cutoff, the value of transitioning parameter is expected to be approximately 90–100%. However, if this value is around 50–65%, it is doubtful whether a distinguishable burst/suppression alternation exists. Furthermore, as both transitions, at the beginning and at the end of the dIBI, are important, we calculate for every dIBI 2 transitioning parameters.

6) NLEO local maxima (one parameter): In some cases, bursts can occur synchronously with relatively low amplitude ($<$10–20 μV) and can be missed. Another common scenario is that a burst is present on less than 50% of EEG channels. This can produce a false merging of two shorter dIBIs into a longer one. To examine the presence of potentially missed bursts, we apply a NLEO as a very effective method for detection of bursts and dynamic EEG activity [14]. NLEO is calculated using the following formula:

$$\psi\left(x\left[n\right]\right) = x^2\left[n\right] - x\left[n-1\right] \cdot x\left[n+1\right].$$

We calculate an average NLEO across all EEG channels and use the maximal value of this signal as the final parameter.

ACKNOWLEDGMENT

The authors would like to thank the patients and their parents for their cooperation and the neurotechnologists who made the high-quality EEG recordings.

REFERENCES

[1] J. E. Lawn, "4 million neonatal deaths: When? Where? Why?" *Lancet*, vol. 365, no. 9462, pp. 891–900, Mar. 2005.

[2] B. Hagberg, "Changing panorama of cerebral palsy in Sweden. VIII. Prevalence and origin in the birth year period 1991–94," *Acta Paediatr.*, vol. 90, no. 3, pp. 271–277, Mar. 2001.

[3] J. H. Richardus, "Differences in perinatal mortality and suboptimal care between 10 European regions: Results of an international audit," *BJOG: Int. J. Obstetrics Gynaecol.*, vol. 110, no. 2, pp. 97–105, Feb. 2003.

[4] N. Monod, "The neonatal EEG: statistical studies and prognostic value in full-term and pre-term babies," *Electroencephalogr. Clin. Neurophysiol.*, vol. 32 no. 5, pp. 529–544, May 1972.

[5] K. Watanabe, "Behavioral state cycles, background EEGs and prognosis of newborns with perinatal hypoxia," *Electroencephalogr. Clin. Neurophysiol.*, vol. 49, no. 5–6, pp. 618–625, Sep. 1980.

[6] C. Pezzani, "Neonatal electroencephalography during the first twenty-four hours of life in full-term newborn infants," *Neuropediatrics*., vol. 17, no. 1, pp. 11–18, Feb. 1986.

[7] E. Biagioni, "Constantly discontinuous EEG patterns in full-term neonates with hypoxic-ischaemic encephalopathy," *Clin. Neurophysiol.*, vol. 110, no. 9, pp. 1510–1515, Sep. 1999.

[8] C. C. Menache, "Prognostic value of neonatal discontinuous EEG," *Pediatr. Neurol.*, vol. 27, no. 2, pp. 93–101, Aug. 2002.

[9] D. M. Murray, "Early EEG findings in hypoxic-ischemic encephalopathy predict outcomes at 2 years," *Pediatrics*, vol. 124, no. 3, pp. 459–467, Aug. 2009.

[10] T. N. Tsuchida, "American clinical neurophysiology society standardized EEG terminology and categorization for the description of continuous EEG monitoring in neonates: Report of the American Clinical Neurophysiology Society critical care monitoring committee," *J. Clin. Neurophysiol.*, vol. 30, no. 2, pp. 161–173, Apr. 2013.

[11] C. T. Lombroso, "Neonatal polygraphy in full-term and premature infants: A review of normal and abnormal findings," *J. Clin. Neurophysiol.*, vol. 2, no. 2, pp. 105–155, Apr. 1985.

[12] I. Korotchikova, "Quantitative EEG analysis in neonatal hypoxic ischaemic encephalopathy," *Clin. Neurophysiol.*, vol. 122, no. 8, pp. 1671–1678, Feb. 2011.

[13] J. Löfhede, "Automatic classification of background EEG activity in healthy and sick neonates," *J. Neural Eng.*, vol. 7, no. 1, Feb. 2010.

[14] K. Palmu, "Detection of 'EEG bursts' in the early preterm EEG: Visual versus automated detection," *Clin. Neurophysiol.*, vol. 121, no. 7, pp. 1015–1022, Jul. 2010.

[15] W. Jennekens, "Automatic burst detection for the EEG of the preterm infant," *Physiol. Meas.*, vol. 32, no. 10, pp. 1623–1637, Sep. 2011.

[16] T. J. Mitchell, "Automating the analysis of EEG recordings from prematurely-born infants: A Bayesian approach," *Clin. Neurophysiol.*, vol. 124, no. 3, pp. 452–461, Sep. 2012.

[17] N. Koolen, "Line length as a robust method to detect high-activity events: Automated burst detection in premature EEG recordings," *Clin. Neurophysiol.*, vol. 125, no. 10, pp. 1985–1994, Feb. 2014.

[18] P. J. Cherian, "Validation of a new automated neonatal seizure detection system: A clinician's perspective," *Clin. Neurophysiol.*, vol. 122, no. 8, pp. 1490–1499, Aug. 2011.

[19] M. De Vos, "Automated artifact removal as preprocessing refines neonatal seizure detection," *Clin. Neurophysiol.*, vol. 122, no. 8, pp. 2345–2354, Dec. 2011.

[20] V. Matic, "Holistic approach for automated background EEG assessment in asphyxiated full-term infants," *J. Neural Eng.*, vol. 11, no. 6, Dec. 2014.

[21] V. Matic, "Objective differentiation of neonatal EEG background grades using detrended fluctuation analysis," *Front. Hum. Neurosci.*, vol. 9, no. 189, Apr. 2015.

[22] V. Krajca, "Automatic identification of significant graphoelements in multichannel EEG recordings by adaptive segmentation and fuzzy clustering," *Int. J. Biomed. Comput.*, vol. 28, no. 1–2, pp. 71–89, May–Jun. 1991.

[23] V. Matic, "Automated EEG inter-burst interval detection in neonates with mild to moderate postasphyxial encephalopathy," in *Proc. IEEE Annu. Int. Conf. Eng. Med. Biol. Soc.*, Aug. 2012, vol. 2012, pp. 17–20..

[24] J. A. Suykens, "Least squares support vector machine classifiers," *Neural Process. Lett.*, vol. 9, no. 3, pp. 293–300, 1999.

[25] K. De Brabanter, "LS-SVMlab Toolbox User's Guide," Katholieke Universiteit Leuven, Leuven, Belgium, ESAT-SISTA Tech. Rep. 10-146, 2010.

[26] S. Xavier-de-Souza, "Coupled simulated annealing," *IEEE Trans. Syst., Man, Cybern. B, Cybern.*, vol. 40, no. 2, pp. 320–335, Apr. 2004.

[27] J. Löfhede, "Classification of burst and suppression in the neonatal electroencephalogram," *J. Neural Eng.*, vol. 5, no. 4, pp. 402–410, Dec. 2008.

[28] A. Flisberg, "Prognostic capacity of automated quantification of suppression time in the EEG of post asphyctic full term neonates," *Acta Paediatr.*, vol. 100, no. 10, pp. 1338–1343. May 2011.

[29] D. B. Sinclair, "EEG and long-term outcome of term infants with neonatal hypoxic-ischemic encephalopathy," *Clin. Neurophysiol.*, vol. 110, no. 4, pp. 655–659, Apr. 1999.

[30] S. Mallat, *A Wavelet Tour Of Signal Processing: The Sparse Way*. New York, NY, USA: Academic, 2008.

[31] B. H. Walsh, "The use of conventional EEG for the assessment of hypoxic ischaemic encephalopathy in the newborn: A review," *Clin. Neurophysiol.*, vol. 122, no. 7, pp. 1284–1294. May 2011.

Authors' photographs and biographies not available at the time of publication.